

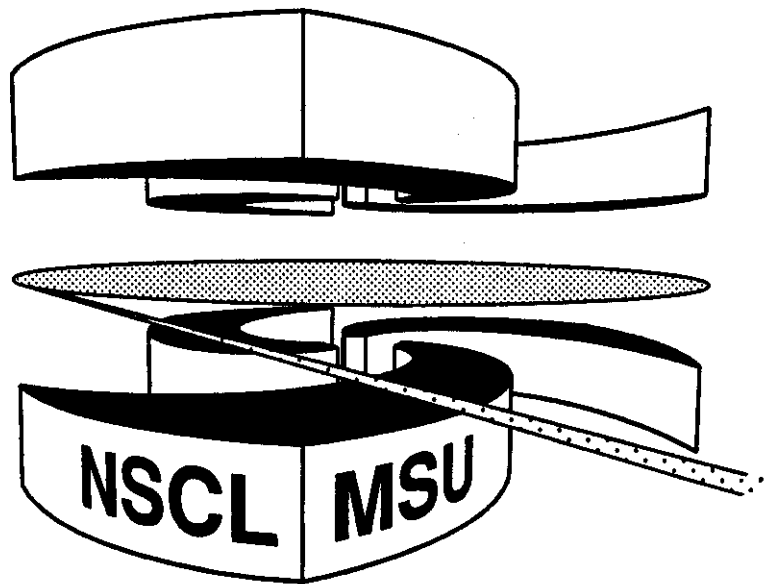


Michigan State University

National Superconducting Cyclotron Laboratory

**NUCLEAR DYNAMICS AND INTENSITY INTERFEROMETRY**

**WOLFGANG BAUER**



**To appear in Nuclear Physics**

# NUCLEAR DYNAMICS AND INTENSITY INTERFEROMETRY

Wolfgang **BAUER**

Department of Physics and Astronomy and  
 National Superconducting Cyclotron Laboratory  
 Michigan State University, **East** Lansing MI 48824-1321, USA

## Abstract

The present status of the use of two-particle intensity interferometry as a diagnostic tool to study the dynamics of intermediate energy heavy ion collisions is examined. Calculations for the two-proton correlation function are presented and compared to experiment. These calculations are based on the nuclear **Boltzmann-Uehling-Uhlenbeck** transport theory. At heavy ion beam energies **around 100 MeV** per nucleon it is found that there is only a weak sensitivity of the results on the nuclear compressibility, but a strong dependence on the in-medium nucleon-nucleon cross section.

## 1. INTRODUCTION

Intensity interferometry was introduced by **Hanbury Brown** and **Twiss** as a technique for astronomical distance measurement [1]. They recorded the two-photon correlation function for incoming coincident photons as a function of their relative momentum. This correlation function can be written as:

$$R(\vec{k}_1, \vec{k}_2) = \frac{\langle n_{12} \rangle}{\langle n_1 \rangle \langle n_2 \rangle} - 1, \quad (1)$$

where  $\langle n_{12} \rangle$  is the probability of detecting two coincident photons of wavenumber  $\vec{k}_1$  and  $\vec{k}_2$  in detectors 1 and 2, and  $\langle n_i \rangle$  is the **probability** of detecting a photon of momentum  $\vec{k}_i$  in detector  $i$  ( $i = 1, 2$ ). Equation 1 contains only count rates, which are proportional to the absolute squares of the amplitudes. As a consequence, HBT interferometry is insensitive to phase shifts introduced by atmospheric disturbances. It can be used with very large base lines and delivers superior resolution. This was **first** shown in [2] by measuring the angular diameter of Sirius.

The physical basis of the HBT effect is that two photons have a non-zero correlation function due to the **symmetrization** of their wave functions, a consequence of the quantum statistics for identical particles.

A similar technique can also be used for source size determinations in subatomic physics. This was **first** realized by Goldhaber et al. [3] by studying angular distributions of pions in  $p\bar{p}$  annihilation processes. **They** found that the emission probability of coincident identical pions is strongly affected by their Bose-Einstein statistics, which causes an enhancement of the correlation function at **zero** relative momentum,  $q = 0$ . **The** width of the maximum at  $q = 0$  depends on the radius of the interaction volume [3] and also on the life-time of the emitting **source** [4].

In recent years, two-pion intensity interferometry has been strongly pursued at ultra-relativistic energies, where the interest is on the interplay between source dynamics and final state interaction [5, 6] and pion correlations from an exploding source [7]. Intensity interferometry derives its main attraction, however, from the prospect of its possible use as a diagnostic tool for the formation of quark-gluon plasma [7, 8].

Intensity interferometry is not restricted to bosons, but can also be applied to Fermions. Koonin [9] proposed to use two-proton intensity interferometry to obtain ‘pictures’ of heavy ion collisions. The advantage of using protons as a probe lies in the fact that they are already present in the colliding nuclei and can be liberated relatively easily. In contrast, to create a pair of pions one has to spend an energy  $E_{\min} = 2m_{\pi} \approx 280$  MeV in the center of mass of the generating system. Therefore, protons can be used as a probe at much lower energies. In addition, the two-proton relative wave function contains the prominent  ${}^2\text{He}$ -‘resonance’, which leads to enhanced sensitivity of the correlation function to the source size. Lastly, protons are easy to detect with the required resolution.

Recent progress has been centered around the theoretical computation of two-proton correlation functions from nuclear transport theory [10, 11, 12, 13]. In this framework, it is now possible to understand the dependence of the correlation functions on the parameters discussed above. Comparisons of this theory to experimental data [10, 12, 13] have now established two-proton intensity interferometry as a quantitative tool to study heavy ion reaction dynamics.

Recently, several groups have begun to study two-neutron correlations [14, 15, 16, 17]. This probe has the advantage that there is no Coulomb interaction between the two neutrons or between the neutrons and the emitting source. However, there are bigger experimental obstacles due to the relatively small neutron detection efficiencies of good-resolution detectors and due to problems associated with ‘cross-talk’ between neighboring detectors.

A summary of the present status of the field as well as further references can be found in [18]. In this paper we will primarily focus on the use of two proton intensity interferometry as a diagnostic tool for studying intermediate energy heavy ion reaction dynamics and with it the determination of limits on the parameters of interactions of nucleons in dense nuclear matter.

## 2. INTERMEDIATE ENERGY HEAVY ION TRANSPORT THEORY

During the last 5-7 years, several groups have developed a nuclear transport theory for intermediate energy ( $20 \text{ MeV} \leq E_{\text{beam}}/A \leq 2 \text{ GeV}$ ) heavy ion reactions [19, 20, 21, 22]. This transport theory describes the time evolution of the nuclear one-body Wigner distribution  $f(\vec{r}, \vec{p}, t)$  under the influence of the nuclear mean field and individual nucleon-nucleon collisions via the Boltzmann-Uehling-Uhlenbeck (BUU) equation

$$\begin{aligned} \frac{\partial}{\partial t} f(\vec{r}, \vec{p}, t) + \frac{\vec{p}}{m} \vec{\nabla}_{\vec{r}} f(\vec{r}, \vec{p}, t) - \vec{\nabla}_{\vec{r}} U \vec{\nabla}_{\vec{p}} f(\vec{r}, \vec{p}, t) & \quad (2) \\ = \frac{g}{2\pi^3 m^2} \int d^3 q_1 d^3 q_2 d^3 q_2' & \\ \delta \left( \frac{1}{2m} (p^2 + q_2^2 - q_1^2 - q_2'^2) \right) \cdot \delta^3(\vec{p} + \vec{q}_2 - \vec{q}_1' - \vec{q}_2') \cdot \frac{d\sigma}{d\Omega} & \\ \cdot \left\{ f(\vec{r}, \vec{q}_1', t) f(\vec{r}, \vec{q}_2', t) (1 - f(\vec{r}, \vec{p}, t)) (1 - f(\vec{r}, \vec{q}_2, t)) \right. & \\ \left. - f(\vec{r}, \vec{p}, t) f(\vec{r}, \vec{q}_2, t) (1 - f(\vec{r}, \vec{q}_1', t)) (1 - f(\vec{r}, \vec{q}_2', t)) \right\}, & \end{aligned}$$

Here  $U$  is the mean field potential, and  $d\sigma/d\Omega$  is the in-medium nucleon-nucleon scattering

cross section.

All present solution schemes for the above equation employ the test particle method, in which the entire phase space is divided into small cells, whose equations of motion are first order differential equations in time. The collision integral is solved via an intranuclear cascade [23] for the test particles. The test particle collisions respect the Pauli exclusion principle due to the presence of the factors  $1 - f$ , which are numerically implemented via a Monte Carlo rejection method.

### 3. LARGE-ANGLE CORRELATIONS

Since the solution of Equation 2 represents the time evolution of the single particle distribution function  $f$ , it is possible (in the limit of  $t \rightarrow \infty$ ) to predict all single particle observables such as proton spectra [24] in this theory. It is also possible to predict the production cross sections of secondary particles such as pions [19, 20, 25] or high-energy photons [26].

Predictions for two-particle correlations can only be made, if these correlations are simply consequences of the conservation laws for momentum, energy, angular momentum, and particle number. We have shown [27] that two-proton correlation functions measured at large angles can be successfully reproduced by the BUU theory, provided that total momentum conservation is correctly taken into account. In another investigation Ardouin et al. [28] found that the variation of the large angle correlation function with polar angle  $\theta$  is largely due to angular momentum effects.

### 4. CALCULATION OF CORRELATIONS AT SMALL RELATIVE MOMENTUM

At small relative momentum  $\vec{q} = \frac{1}{2}(\vec{p}_1 - \vec{p}_2)$ , the interaction between the two particles has to be taken into account explicitly to calculate the two-particle correlation function.

To derive an expression for the two-particle correlation function,  $C(\vec{P}, \vec{q})$ , we assume that the final-state interaction between the two detected particles dominates, that final-state interactions with all remaining particles can be neglected, that the correlation functions are determined by the two-body density of states as corrected by the interactions between the two particles, and that the single particle phase space distribution function of emitted particles,  $g(\vec{p}, x)$  varies slowly as a function of momentum  $\vec{p}$  (i.e.  $g(\vec{p}, x) \approx g(\vec{p} \pm \vec{q}, x)$ ). Then the theoretical expression for the two-particle correlation function can be written as [9, 7, 11]

$$C(\vec{P}, \vec{q}) = R(\vec{P}, \vec{q}) + 1 = \frac{\Pi_{12}(\vec{p}_1, \vec{p}_2)}{\Pi_1(\vec{p}_1)\Pi_1(\vec{p}_2)} = \frac{\int d^4x_1 d^4x_2 g(\frac{1}{2}\vec{P}, x_1)g(\frac{1}{2}\vec{P}, x_2) \left| \phi\left(\vec{q}, \vec{r}_1 - \vec{r}_2 + \frac{\vec{P}(t_2 - t_1)}{2m}\right) \right|^2}{\int d^4x_1 g(\frac{1}{2}\vec{P}, x_1) \int d^4x_2 g(\frac{1}{2}\vec{P}, x_2)}, \quad (3)$$

where  $\vec{P} = \vec{p}_1 + \vec{p}_2$  is the total momentum of the particle pair.  $x_1$  and  $x_2$  are the space-time points of the emission of protons 1 and 2.  $\Pi_1$  is the single- and  $\Pi_{12}$  is the two-particle emission probability.

$\phi(\vec{q}, \vec{r})$  is the relative wave function of the particle pair. The effect that gives rise to the HBT effect is the identical particle interference. In the absence of any other interaction the square of

the two particle wave function is then simply given by

$$|\phi(\vec{q}, \vec{r})|^2 = 1 \pm \cos(2\vec{q}\vec{r}), \quad (4)$$

where the upper sign stands for bosons and the lower for fermions.

In the presence of other interactions this result is modified. The relative wave function for Coulomb scattering is

$$\phi_c(\vec{q}, \vec{r}) = \exp(-\frac{1}{2}\pi\eta) \Gamma(1 + i\eta) \exp(iqz) {}_1F_1(-i\eta|1|iq(r-z)) \quad (5)$$

where  ${}_1F_1$  is the confluent hypergeometric series, and  $\eta = \alpha Z_1 Z_2 m_\pi / q$ . The two-pion relative wave function at small relative momentum is usually approximated as the symmetrized Coulomb scattering wave function

$$|\phi_{\pi\pi}(\vec{q}, \vec{r})|^2 = \frac{1}{2} |\phi_c(\vec{q}, \vec{r}) + \phi_c(\vec{q}, -\vec{r})|^2 \quad (6)$$

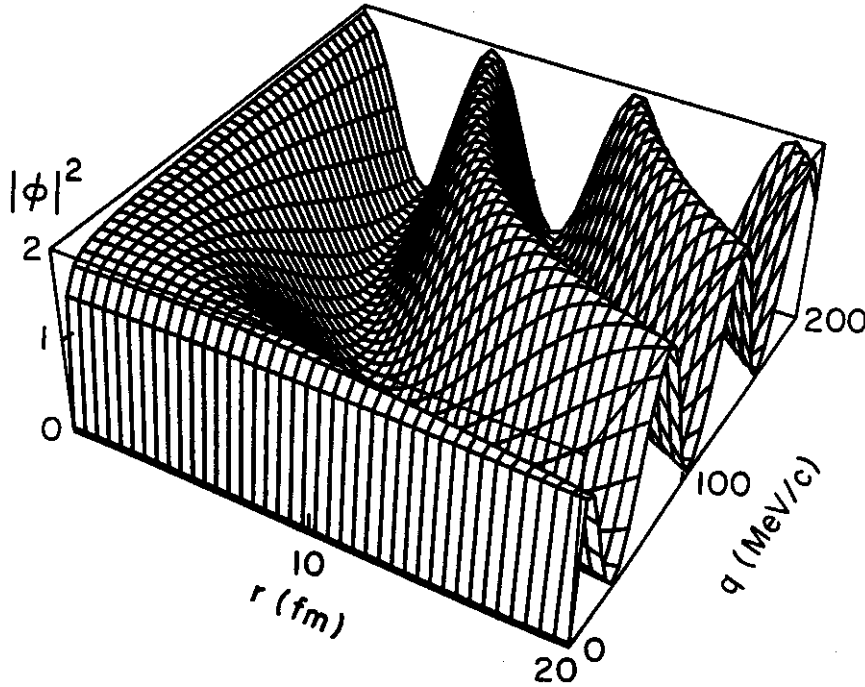


Figure 1: Absolute square of the two-pion relative wave function,  $|\phi_{\pi\pi}(q, r, \cos \theta = 0.5)|^2$ .

Due to symmetries, the wave function only depends on three independent variables which we choose to be  $q$ ,  $r$ , and  $\cos \theta = \vec{q} \cdot \vec{r} / qr$ . The square of the two-pion relative wave function is displayed in Figure 1 as a function of  $q$  and  $r$  for  $\cos \theta = 0.5$ . For  $r \rightarrow 0$ ,  $|\phi_{\pi\pi}|^2$  is now given by the the Gamov penetration factor

$$|\phi_{\pi\pi}(\vec{q}, 0)|^2 = 2 \frac{2\pi\eta}{\exp(2\pi\eta) - 1} \quad (7)$$

For the two-proton relative wave function the strong interaction with the prominent  ${}^2\text{He}$ -'resonance' cannot be neglected. To obtain the relative wave function in this case, we solve a

radial Schrödinger equation with the Coulomb and the modified Reid soft core potential. The two-proton relative wave function is shown in Figure 2. One can observe the peak at  $q \approx 20$  MeV/c due to the  ${}^2\text{He}$ -'resonance'. Due to the effect of antisymmetrization,  $|\phi_{pp}| \rightarrow 0$  as  $r \rightarrow 0$ .

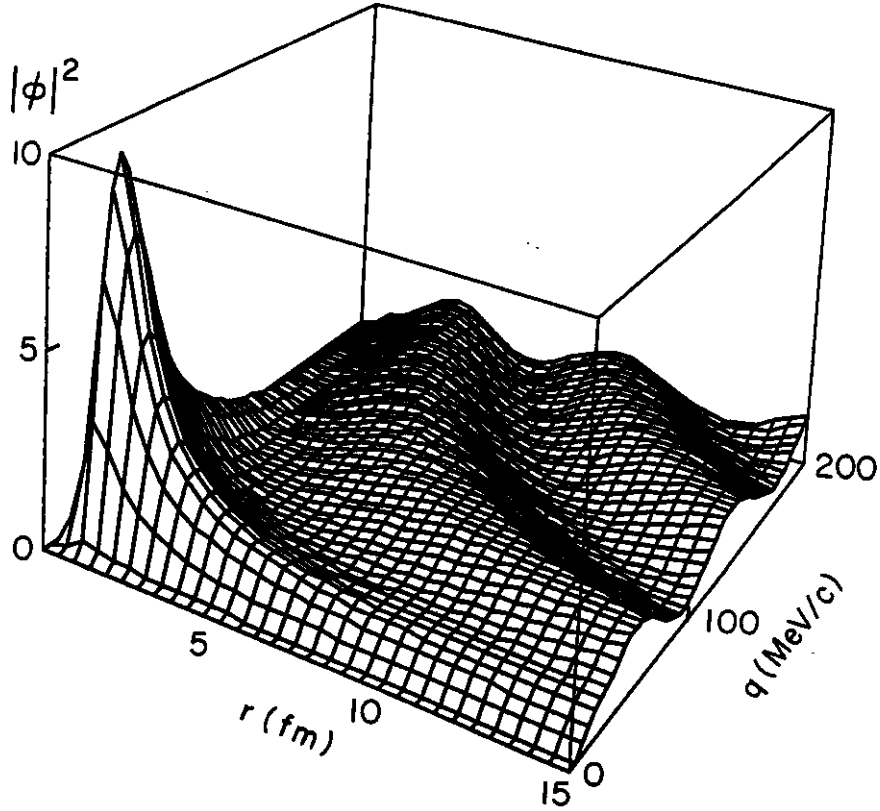


Figure 2: Absolute square of the two-proton relative wave function,  $|\phi_{pp}(q, r, \cos \theta = 0.5)|^2$ .

Equation 3 requires only the two-particle relative wave function and the *single*-particle phase space distribution function. Under the assumptions stated above it is thus possible to generate *two*-particle correlation functions for small relative momenta from a theory which only predicts *one*-particle distribution functions.

The resulting two-particle correlation function contains information on the emitting source. To see this, we rewrite Equation 3 as

$$C(\vec{P}, \vec{q}) = \int d^3r F_P(\vec{r}) |\phi(\vec{q}, \vec{r})|^2. \quad (8)$$

Here  $\vec{r} = \vec{r}_1 - \vec{r}_2$  is the relative coordinate of the two emitted particles, and the function  $F_P(\vec{r})$  is defined as

$$F_P(\vec{r}) = \frac{\int d^3R f(\frac{1}{2}\vec{P}, \vec{R} + \frac{1}{2}\vec{r}, t_>) f(\frac{1}{2}\vec{P}, \vec{R} - \frac{1}{2}\vec{r}, t_>)}{\left( \int d^3r f(\frac{1}{2}\vec{P}, \vec{r}, t_>) \right)^2}, \quad (9)$$

where  $\vec{R} = \frac{1}{2}(\vec{r}_1 + \vec{r}_2)$  is the center-of-mass coordinate of the two particles, and the Wigner function  $f(\vec{p}, \vec{r}, t_>)$  is the phase space distribution of particles with momentum  $\vec{p}$  and position  $\vec{r}$  at some time  $t_>$  after both particles have been emitted:

$$f(\vec{p}, \vec{r}, t_>) = \int_{-\infty}^{t_>} dt g(\vec{p}, \vec{r} - \vec{p}(t_> - t)/m, t). \quad (10)$$

For a given momentum  $\vec{P}$ , the correlation function has three degrees of freedom,  $\vec{q}$ , which are a function of  $F_{\vec{P}}(\vec{r})$ . Therefore correlation function measurements should allow the extraction of  $F_{\vec{P}}(\vec{r})$ , the normalized probability of two protons with the same momentum  $\vec{P}/2$  being separated by  $\vec{r}$ .

One may also use correlation function measurements to test various theoretical models capable of predicting  $g(\vec{p}, \vec{r}, t)$  and thus making specific predictions about the correlation functions. This approach is more realistic in its goals as a full six-dimensional determination of  $C(\vec{P}, \vec{q})$  is very difficult in practice.

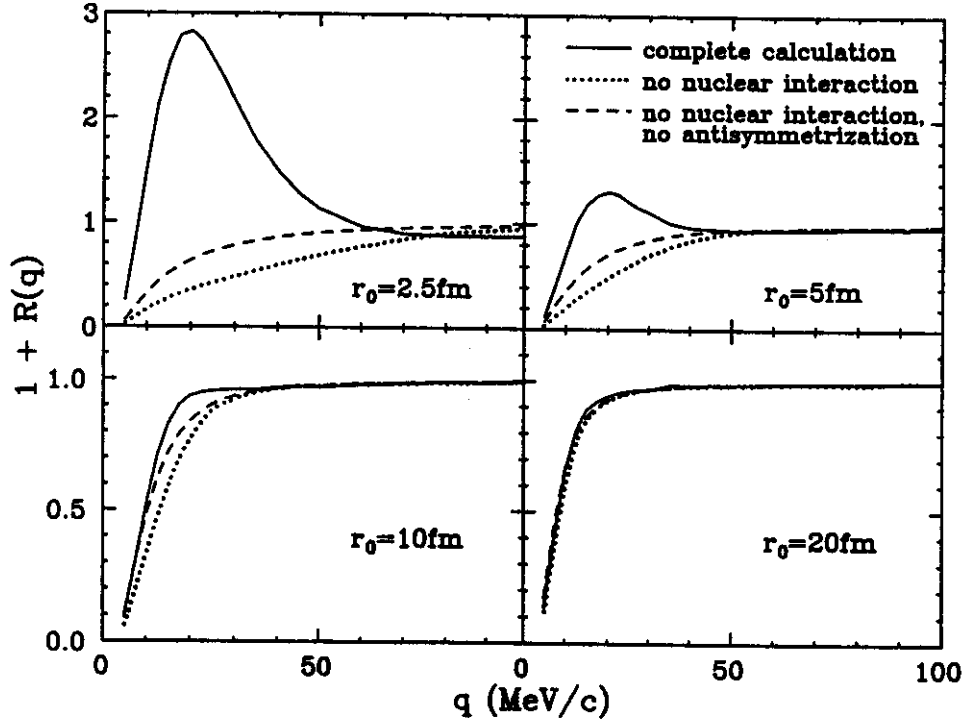


Figure 3: Two-proton correlation functions calculated with a source parameterization according to Equation 11. The solid lines represent the complete calculations including the effects of quantum statistics and of the Coulomb and strong interaction. The dashed lines represent the case of only Coulomb interaction, and the dotted line is for Coulomb interaction plus the effect of the Fermi-Dirac statistics for the two protons. (From [11])

## 5. SENSITIVITY OF THE TWO-PROTON CORRELATION FUNCTION

It is instructive to examine the sensitivity of the two-particle correlation function to different components of the two-particle interaction. We perform such a study for the two-proton correlation function. To do this, we use a simple zero-lifetime Gaussian source parameterization

$$g_0(\vec{p}, \vec{r}, t) = \rho_0 \exp(-r^2/r_0^2) \delta(t - t_0), \quad (11)$$

where  $r_0$  is the radius of the source. Figure 3 illustrates the effects of the different contributions to the two-proton final state interaction for sources of different radii. The Coulomb interaction

dominates the shape of the correlation function for very large source radii. For  $r_0 < 20$  fm, the correlation function becomes increasingly sensitive to the effects of antisymmetrization and the strong interaction. The strong interaction has the dominant effect for source radii around  $r_0 = 2.5$  fm due to the prominent  ${}^2\text{He}$  resonance.

It should be pointed out at this point, however, that in a realistic calculation the use of a simple zero life-time Gaussian source parametrization is not sufficient [18]. Instead, calculations containing the full time and momentum dependence of the emitting source are needed.

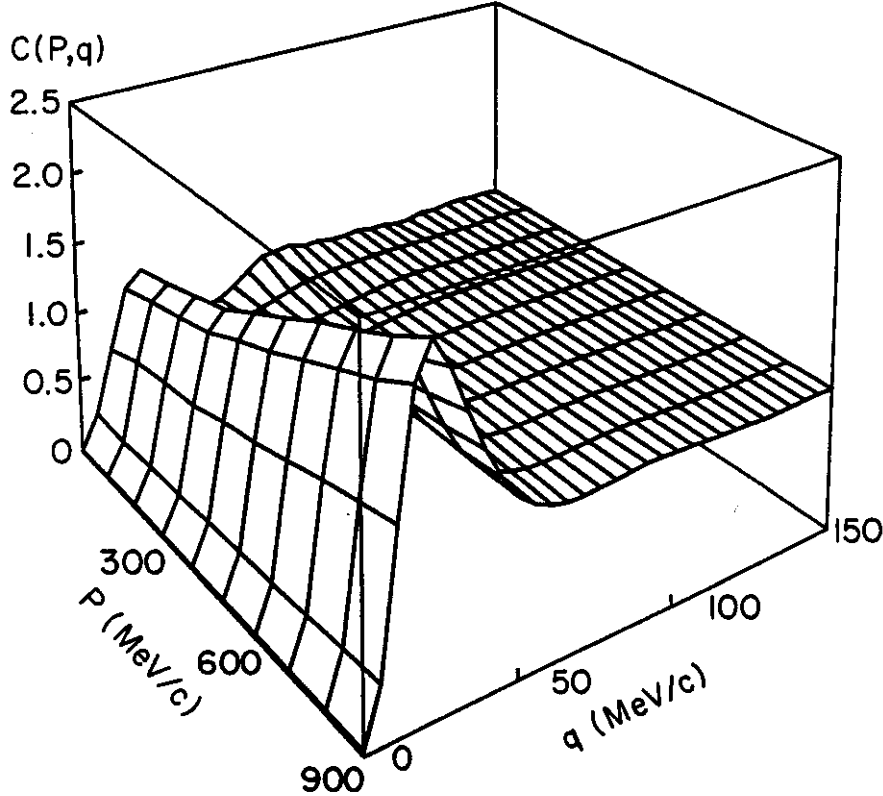


Figure 4: Two-proton correlation function as a function of the absolute value of total pair momentum,  $P$ , and relative momentum,  $q$ , for the reaction  ${}^{14}\text{N} + {}^{27}\text{Al}$  at beam energy  $E/A = 75$  MeV and impact parameter  $b = 0$  fm.

## 6. CALCULATION OF TWO-PROTON CORRELATION FUNCTIONS

We perform calculations of the single particle phase space distribution function  $f(\vec{r}, \vec{p}, t)$  by numerically solving Equation 2. These single particle distributions are then inserted into Equation 3 to generate the two-particle correlation function at small relative momentum.

In Figure 4, we show the two-proton correlation function,  $C(P, q)$ , calculated for the reaction  ${}^{14}\text{N} + {}^{27}\text{Al}$  at beam energy  $E/A = 75$  MeV and impact parameter  $b = 0$  fm. We can clearly observe the suppression of the correlation function at  $q \approx 0$  due to the combined effects of Coulomb interaction and antisymmetrization. Also clearly visible is the enhancement of the correlation function around  $q = 20$  MeV/c due to the  ${}^2\text{He}$  resonance. One can see that the height of the resonance peak varies with total momentum,  $P$ . This effect is also experimentally observed. When using Equation 11 to fit a source radius to the correlation function one then observes a typical momentum dependence of the extracted source size.



One effect that may be responsible for this behavior is cooling of the source [29]. As a consequence of the falling temperature, the characteristic lifetime for high-energy particles is much shorter than the one for low-energy ones [11], leading to the observed effect. It is therefore clear that meaningful interpretations of the two-proton correlation function require, in general, calculations capable of predicting the full space-time dependence of the emission function.

In Figure 5, we show the dependence of the height of the peak in the correlation function,  $C(P, q=20 \text{ MeV})$ , as a function of impact parameter and total pair momentum. We predict a rich structure, which can and will be studied experimentally by using  $4\pi$  detector systems for impact parameter triggering.

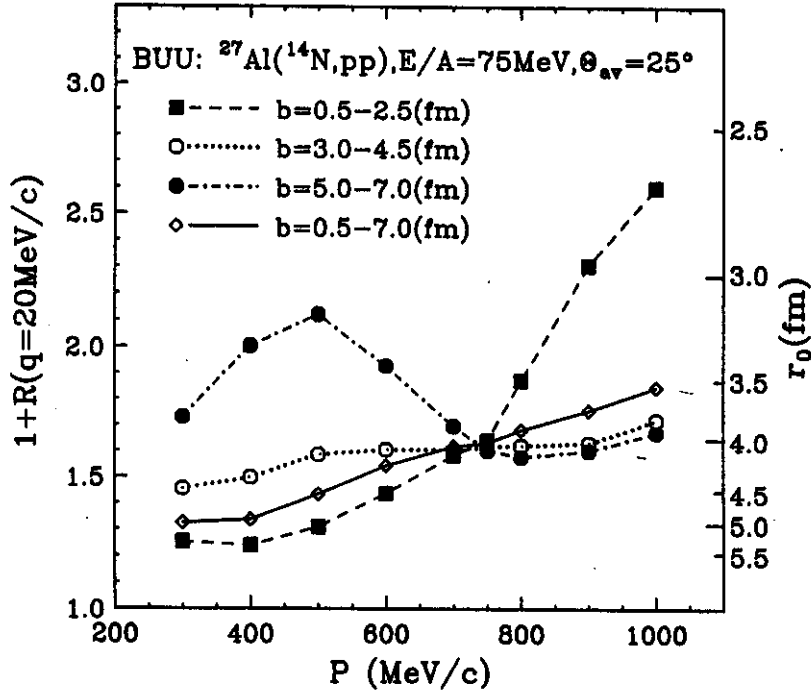


Figure 5: Pair momentum and impact parameter dependence of the height of the maximum of the two-proton correlation function for the reaction  $^{14}\text{N} + ^{27}\text{Al}$  at  $E/A = 75 \text{ MeV}$ , as predicted by calculations based on the BUU theory. (From [11])

## 7. COMPARISON WITH EXPERIMENT

In Figure 6, we compare our calculations of the two-proton correlation function to experimental data for the system  $^{14}\text{N} + ^{27}\text{Al}$  at a beam energy of  $E/A = 75 \text{ MeV}$ . Since the experimental data were not triggered on impact parameter, we have to also integrate our calculations over impact parameter with the proper weighting factors. (Details of this impact parameter averaging can be found in the Appendix of [12].) The experimental and theoretical correlation functions are shown as a function of the relative momentum  $q$  for three different gates on the total pair momentum  $|\vec{P}| = |\vec{p}_1 + \vec{p}_2|$ . For comparison, the beam momentum per nucleon is  $p_{\text{beam}} \approx 375 \text{ MeV}/c$ .

We show two different calculations. The solid line represents the full BUU calculations with the full nucleon-nucleon cross sections. The dotted line is the result of the BUU calculation with a reduced in-medium cross section,  $\sigma = \frac{1}{2}\sigma_{nn}$ , where  $\sigma_{nn}$  is the free space elementary nucleon-nucleon cross section. In both cases the medium corrections due to the Pauli-principle for the final nucleon scattering states are, of course, taken into account.

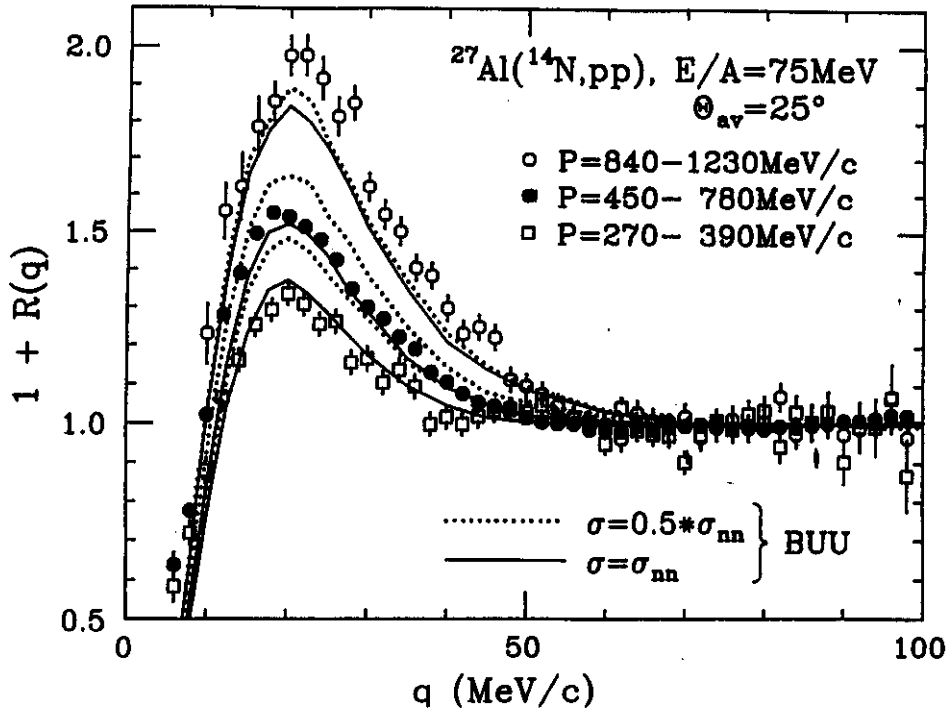


Figure 6: Two-proton correlation function for the reaction  $^{14}\text{N} + ^{27}\text{Al}$  at  $E/A = 75$  MeV, as predicted by calculations based on the BUU theory (lines) and as experimentally measured (plot symbols). (From [12])

It is clear from this figure that sizeable differences between the two calculations with different assumptions on the in-medium nucleon-nucleon cross section exist. In fact, variations of the cross section by only 10% result in differences between the calculated correlation functions which should be experimentally measurable. From this one has to conclude that two-particle correlation functions are very sensitive probes for the collisional dynamics of intermediate energy heavy ion collisions.

In Figure 7 we display the sensitivity of the two-proton correlation function to the in-medium nucleon-nucleon cross section,  $\sigma$ , and to the value of the nuclear matter compressibility,  $\kappa$ . We show the results of our calculations for a stiff nuclear equation of state ( $\kappa = 380$  MeV) and different values of the in-medium nucleon-nucleon cross section.

From our theoretical results and comparisons to experimental data we conclude that the value of the in-medium cross section (without correction due to the final state 'Pauli blocking') is very close to the experimentally measured (energy dependent) free value. This is in agreement with information we extracted from our investigation of the disappearance of nuclear collective flow [30, 31]

We also varied the compressibility of nuclear matter, which enters the calculations through the density dependence of the mean field potential  $U$ . In Figure 7, we also show a calculation for a soft equation of state ( $\kappa = 200$  MeV). Here we find, however, only a weak sensitivity

of our results on this parameter. This is expected, because for the relatively light system and low beam energy considered here only moderate maximum values of the nuclear density are achieved.

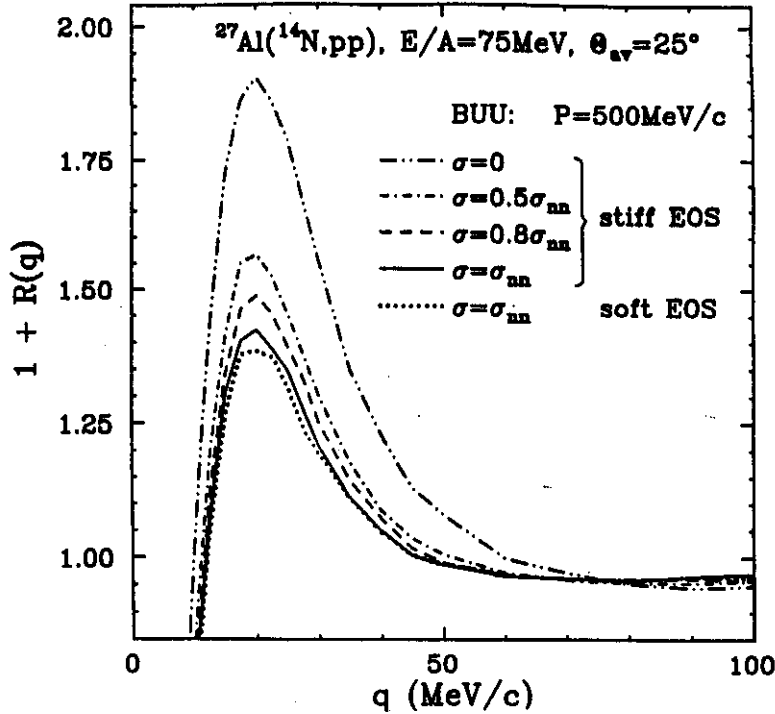


Figure 7: Sensitivity of the two-proton correlation function to the in-medium nucleon-nucleon cross section,  $\sigma$ , and to the nuclear compressibility. (After [10]).

## 8. CONCLUSIONS

The calculation of two-particle correlation functions at small relative momentum on the basis of one-body transport theories is feasible by using the convolution techniques described above. Thus intensity interferometry is a powerful tool to test nuclear transport theories and to investigate nuclear dynamics.

Comparisons with experiment show that the BUU transport theory is able to reproduce detailed features of the experimentally measured two-proton correlation functions. These features include the pair momentum dependence of the peak due to the  ${}^2\text{He}$ -‘resonance’, the effect of source deformation, and the lifetime effect on the correlation function.

We have shown that the theoretically obtained two-proton correlation functions are sensitive to the value of the in-medium nucleon-nucleon cross section. At higher beam energies and for large systems we also expect a sensitivity of the results on the compressibility of nuclear matter. Thus nuclear intensity interferometry is a useful tool to investigate the nuclear transport properties, and it should also enable us to conduct further studies of the nuclear equation of state.

From a theoretical standpoint it would clearly be desirable to compare to impact parameter resolved experimental data, which would further increase the sensitivity of two-particle

correlation functions at small relative momentum to the effects discussed above.

This work was supported by the National Science Foundation under Grants No. 89-06116 and 90-17077. Helpful conversations and collaborations with G.F. Bertsch, P. Danielewicz, C.K. Gelbke, W.G. Gong, and S. Pratt are gratefully acknowledged.

## REFERENCES

- [1] R. Hanbury Brown and R.Q. Twiss, *Phil. Mag.* **45** (1954) 663.
- [2] R. Hanbury Brown and R.Q. Twiss, *Nature* **178** (1956) 1046.
- [3] G. Goldhaber, S. Goldhaber, W. Lee, and A. Pais, *Phys. Rev.* **120** (1960) 300.
- [4] E.V. Shuryak, *Phys. Lett.* **B44** (1973) 387.
- [5] S. Pratt, *Phys. Rev. Lett.* **53** (1984) 1219.
- [6] K. Kohlemainen, and M. Gyulassy, *Phys. Lett.* **B180** (1986) 203.
- [7] S. Pratt, *Phys. Rev.* **D33** (1986) 1314.
- [8] G. Bertsch, M. Gong, and M. Tohyama, *Phys. Rev.* **C37** (1988) 1896.
- [9] S.E. Koonin, *Phys. Lett.* **B70** (1977) 43.
- [10] W.G. Gong, W. Bauer, C.K. Gelbke *et al.*, *Phys. Rev. Lett.* **65** (1990) 2114.
- [11] W.G. Gong, W. Bauer, C.K. Gelbke, and S. Pratt, *Phys. Rev.* **C43** (1991) 781.
- [12] W.G. Gong, W. Bauer, C.K. Gelbke *et al.*, *Phys. Rev.* **C43** (1991) 1804.
- [13] F. Zhu, W.G. Lynch, T. Murakami *et al.*, *Phys. Rev.* **C44** (1991) R582.
- [14] Yu.D. Bayukov, P.V. Degtyarenko, Yu.V. Efremenko *et al.*, *Phys. Lett.* **B189** (1987) 291.
- [15] S.E. Koonin, W. Bauer, and A. Schäfer, *Phys. Rev. Lett.* **62** (1989) 1247.
- [16] W. Dünneweber, W. Lippich, D. Otten, *et al.*, *Phys. Rev. Lett.* **65** (1990) 297.
- [17] B. Jakobsson, B. Norén, A. Oskarsson *et al.*, *Phys. Rev.* **C44** (1991) R1238.
- [18] W. Bauer, C.K. Gelbke, and S. Pratt, *Ann. Rev. Nucl. Part. Sci.* **42** (1992).
- [19] G.F. Bertsch, H. Kruse, and S. Das Gupta, *Phys. Rev.* **C29** (1984) 673.
- [20] H. Kruse, B.V. Jacak, and H. Stöcker, *Phys. Rev. Lett.* **54** (1985) 289.
- [21] C. Grégoire, B. Remaud, F. Scheuter, and F. Sébille, *Nucl. Phys.* **A436** (1985) 365.
- [22] S.J. Wang, B.A. Li, W. Bauer, J. Randrup, *Ann. Phys. (N.Y.)* **209** (1991) 251.
- [23] J. Cugnon, T. Mizutani, and J. Vandermeulen, *Nucl. Phys.* **A352** (1981) 505.
- [24] J. Aichelin and G. Bertsch, *Phys. Rev.* **C31** (1985) 1730.
- [25] B.-A. Li and W. Bauer, *Phys. Lett.* **B254** (1991) 335;  
B.-A. Li and W. Bauer, *Phys. Rev.* **C44** (1991) 450.
- [26] W. Bauer, G.F. Bertsch, W. Cassing, U. and Mosel, *Phys. Rev.* **C34** (1986) 2127.
- [27] W. Bauer, *Nucl. Phys.* **A471** (1987) 604.
- [28] D. Ardouin, Z. Basrak, P. Schuck *et al.*, *Z. Phys.* **A329** (1988) 505 and *Z. Phys.* **A329** (1988) 505.
- [29] D.H. Boal and H. DeGuise, *Phys. Rev. Lett.* **57** (1986) 2901.
- [30] D. Krofcheck, W. Bauer, G.M. Crawley *et al.*, *Phys. Rev. Lett.* **63** (1989) 2028.
- [31] C.A. Ogilvie, W. Bauer, D.A. Cebra *et al.*, *Phys. Rev.* **C42** (1990) R10.